Large-scale 3D flow investigations around a cyclically breathing thermal manikin in a 12 m³ room using HFSB and STB

A. Schröder[1*], D. Schanz[1], J. Bosbach[1], M. Novara[1], R. Geisler[1], J. Agocs[1], A. Kohl[2]
1: German Aerospace Center (DLR), Inst. of Aerodynamics and Flow Technology, Dept. Experimental Methods, Göttingen, Germany
2: German Aerospace Center (DLR), Inst. of Aerodynamics and Flow Technology, Dept. Ground Vehicles, Göttingen, Germany
*andreas.schroeder@dlr.de

Abstract

Exhalation of small aerosol droplets and their transport, dispersion and (local) accumulation in closed rooms have been identified as the main pathway for indirect or airborne respiratory virus transmission from person to person, e.g. for SARS-CoV 2 or measles (Morawska and Cao 2020). Understanding airborne transport mechanisms of viruses via small bio-aerosol particles inside closed populated rooms is an important key factor for optimizing various mitigation strategies (Morawska et al. 2020), which can play an important role for damping the infection dynamics of any future and the ongoing present pandemic scenario, which unfortunately, is still threatening due to the spreading of several SARS-CoV2 variants of concern, e.g. *delta* (Kupferschmidt and Wadman 2021). Therefore, a large-scale 3D Lagrangian Particle Tracking experiment using up to 3 million long lived and nearly neutrally buoyant helium-filled soap bubbles (HFSB) with a mean diameter of ~ 370 µm as passive tracers in a 12 m³ generic test room has been performed, which allows to fully resolve the Lagrangian transport properties and flow field inside the whole room around a cyclically breathing thermal manikin (Lange et al. 2012) with and without mouth-nose-masks and shields applied. Six high-resolution CMOS streaming cameras, a large array of powerful pulsed LEDs have been used and the Shake-The-Box (STB) (Schanz et al. 2016) Lagrangian particle tracking algorithm has been applied in this experimental study of internal flows in order to gain insight into the complex transient and turbulent aerosol particle transport and dispersion processes around seated breathing persons.

Introduction

An enhanced understanding of the transient, turbulent and partly laminar dynamics of Lagrangian transport processes of aerosol particles around cyclically breathing persons with and without protective masks or shields in closed rooms at full temporal and spatial resolution is desired for estimating the risk for infecting other persons in the same room during a specific time span and for implementing proper technical mitigation strategies against the spreading of respiratory viruses, especially SARS-CoV-2. Speaking, singing and coughing generate a large number of variously sized aerosols (Johnson et al. 2011, Fenneley 2020) and an animal study with airborne influenza virus using ferrets indicates effective transmission of viruses in aerosols larger than 1.5 µm (Zhou et al. 2018). The virus load or the number of viral particles in droplets and aerosols is determined by the location of their generation in the infected human airways and by the size of the carrier droplet or aerosol. SARS-CoV-2 is only about 0.08 to 0.12 µm in diameter but is carried through the air in particles of respiratory fluid, which differ in size between 0.2µm and 100µm. While the larger aerosol droplets follow ballistic pathways towards the floor within less than a second, it can be shown for droplets smaller than ~20 µm that the liquid phase evaporates during the time span between exhalation and settling under typical indoor conditions and the remaining aerosol particle diameter can shrink down to less than 5 µm thus becoming an almost passive tracer within the typical mixed convective flow regimes. Recent studies demonstrated that highly infectious Covid-19 patients exhale up to a million of SARS-CoV-2 RNA copies per hour into the air (Ma et al. 2020) while the critical number of inhaled viruses with contact to human airway cells (Zuo et al. 2020) is around a few hundred to one thousand for a 50 % risk of getting infected (Lelieveld et al. 2020), which also depends on the present virus variant. Infectious SARS-CoV-2 virions can be found as well in aerosol particles with a diameter down to 0.25 - 0.5 µm (Liu et al. 2020). Aerosol particles < 5 µm can follow the internal airflow for several minutes and

even up to hours depending on the present buoyancy or pressure forcing in the flow while the settling time for aerosol particles < 2µm in air is even in the order of hours for quiescent air and a height of 2 m.

More recently, a study clarified the reasons for seemingly contradictory results from various, partly clinical studies on the effectiveness of masks against transmission of airborne viruses (Cheng et al. 2021). They concluded that masks are a very effective measure for preventing respiratory virus infections in closed rooms especially when the concentration of virus laden aerosols in the room is limited and/or the residence time of persons inside such rooms is relatively short, while FFP2/3 masks are showing a significant protection gain in comparison to surgical masks or even simpler mouth-nose-masks. Infections despite wearing surgical masks in clinical studies happened almost always in closed rooms with heavy virus loads and/or via accumulation of inhaled virions over longer time-spans. Other studies based on epidemiological data showed as well a clear effectiveness of masks against infections with SARS-CoV-2 in daily usage scenarios (Mitze et al. 2021). While masks are without doubts most effective against airborne virus transmission, as they retain droplets and aerosols directly at the place of exhalation and inhalation, (mobile) air cleaning technologies come next in a row of mitigative measures and should be seriously considered as an additional infection risk reduction device (Curtius et al. 2020, Kähler et al. 2020). They do not rely on human behavior and can help reducing infection risks in occupied places, in addition to wearing protective masks or where it is not possible or problematic to wear masks, that is, in nurseries, classrooms, offices, restaurants and other places.

Based on the gained knowledge from recent worldwide research activities on airborne transmission of SARS-CoV-2 viruses between humans in closed rooms with and without wearing masks or other mitigation measures it is still of specific high interest to understand in detail the Lagrangian transport processes and pathways of small aerosol particles exhaled by a human source including their dispersion and accumulation characteristics. Over longer time spans a local and global accumulation of virus laden aerosols can occur in confined rooms while the SARS-CoV-2 virus has been proven to be stable in airborne particles with a half-life time of more than one hour (van Doremalen et al. 2020). Therefore, it is possible that sharing the same room with an infectious person even under ventilated or limited virus load conditions can lead to inhaling a critical number of viruses over several minutes or even hours accumulatively. Consequently, the governing unsteady and large-scale fluid dynamics inside a whole room is still of major interest: Depending on the location of the spreading source, on the specific constellation of the room geometry, furniture positions, persons and their dynamics and on employing active or passive ventilation inside such confined rooms the resulting dynamic spatial distribution of aerosol particles changes significantly. Therefore, volumetric flow measurements with sufficient temporal resolution are needed to enhance the understanding of the related aerosol particle transport mechanisms. The measurement technique has to be capable of capturing all relevant scales starting from the impulsive and jet-like individual cycles of in– and exhalation over medium scale turbulent transport and diffusion processes in wakes and plumes up to the largest (and slowest) flow-scale circulations in the full room. Existing probe-based measurement methods using detection of gaseous tracers emitted at a potential source position need to rely on statistics at some individual measurement positions while the pathways from the source to the measurement points is kept unknown. The Lagrangian aerosol particle transport inside a populated room is mainly governed by temperature gradients- or buoyancy driven flows (body heat plume, heating systems, electric devices, open windows, stratification etc.), pressure gradient driven flows (open doors and/or windows on opposite sides, active ventilation systems etc.) and by transient and mainly turbulent flows caused by the individual cyclically breathing, speaking, singing etc. events and active movements of persons. As a result, a complex multi-scale and partly turbulent flow situation develops. In order to optimize mitigation concepts for airborne transmission of viruses all mentioned flow properties need to be understood in detail. As a first step the flow in a generic and idealizedroom with a seated and cyclically breathing thermal manikin has been investigated in the present study: Therefore, a large-scale 3D Lagrangian Particle Tracking (LPT) experiment enabling the instantaneous tracking of up to ~3 million submillimeter helium-filled-soap-bubbles (HFSBs) representing the small aerosol particles as passive tracers in a 12 m³ generic test room has been performed at DLR Göttingen in the framework of the project Aeromask, which allows to fully resolve the flow field in the complete room around the manikin.

Set-up and procedure

Six high-resolution CMOS streaming cameras, a large array of powerful pulsed LEDs, four HFSB generator nozzles and the Shake-The-Box (Schanz et al. 2016) LPT algorithm have been combined in this large-scale volumetric experimental study (see Fig. 1, 2 and 3). Based on the reconstructed dense HFSB trajectories covering the complete room volume the related Lagrangian particle transport and dispersion processes are captured over the whole time series of ~52 sec for each test case. Furthermore, many insights into the complex transient and turbulent flow features around the breathing manikin have been discovered after application of the FlowFit data assimilation scheme (Gesemann et al. 2016).

The manikin's surface has been heated homogenously to ~36° C by ~80 W electric power through equidistantly placed heating wires winded around the manikins' body. The manikin has got tailored black clothes and "hair" in order to create a realistic setting and reduce the light reflections from the pulsed LED array. The black clothing led to a specific surface temperature distribution (see infrared camera images in Figure 3 (middle)). In our studies various breathing and coughing scenarios driven by a programmable artificial lung, basically a software controlled motorized piston connected with a hose to the mouth of the 3D printed dummy head (for details see Kohl 2020) have been investigated. Breathing with and without protective measures creates different fluid dynamical interactions with the thermal plume induced by the heated manikin. For each in- and exhaling cycle, measurements were conducted with and with-out an applied mask, a face-shield or a plane acrylic glass shield placed approx. 60 cm in front of the dummy's face (see Fig. 4). All potentially light reflective surfaces and backgrounds have been covered by black curtain or self-adhesive foil (see. Fig 1 (left)).

Figure 1: Experimental set-up at 12 m³ glass room with seated manikin, LED-array and imaging system with six high-resolution CMOS cameras (left) and calibration target on honeycomb material aligned with laser levels (right)

The camera system consisted of 4 x 50 MPx (LaVision Imager MX 50M) and 2 x 25 MPx (AVT Bonito PRO X-2620) global shutter CMOS cameras equipped with Scheimpflug mounts from LaVision and Nikon lenses with a focal length of f = 50 mm at aperture number of $f_{\#}$ = 16, each connected by four CoaXPress cables to frame grabbers of two acquisition PCs. One PC was connected to the four Imager MX 50M cameras and used the DaVis10 acquisition software, which as well controled a PTU (Programmable Timing Unit) from LaVision for synchronization of LED pulses and camera image acquisitions. The other PC was connected to the two AVT cameras and used a self-adapted acquisition software based on the provided AVT software development kit. The camera system allowed almost full views through the whole volume by each of the 50 Mpx cameras and two overlapping part-volume views by the two 25 Mpx cameras, the latter placed in the center of the aligned camera set-up (see Fig. 1 (left)). Only small shadow regions behind the manikin and its legs could not be captured volumetrically. The cameras have been 3D calibrated by using the images of a large planar dot marker target (2.5 m x 1.25 m) (see Fig 1 (right)) at two planes separated in depth by 1.0 m for gaining 3D -2D point correspondences for all camera views. In a second step, a Volume Self Calibration (VSC) procedure (Wieneke 2008) based on particle images of a sparse distribution of HFSBs inside the room and a subsequent Optical Transfer Function (OTF) determination of each camera and sub-volume (Schanz et al. 2012) have been performed. The use of wide angle lenses, as well as a slight waviness of the thin plexiglass wall

induced small decalibrations in the of up to 0.3 px that were not correctable by the used second order camera model. A two-dimensional B-spline corrector field was calibrated for each camera using the averaged differences between the reprojected and the detected real peaks (see Schanz et al. 2019). Using this corrector field the camera errors could be corrected well below 0.1 px. Before each measurement sequence several millions of long-lived and nearly neutrally buoyant helium-filled-soap-bubbles (HFSB) (Bosbach et al. 2009) with ~370 µm mean diameter and ~1.5 mm/sec settling velocity have been homogenously introduced into the room using four flush mounted generator nozzles in the back wall of the room, connected to a LaVision HFSB generator (see Fig 2 (left)). The geometry of the HFSB nozzle and shadow-graphic images of the bubble generation can be found in Fig. 2 (middle). In order to increase the half-life time of the bubbles to approx. 3.75 min we developed an in-house bubble fluid solution. This half-life time corresponds to a time-constant tau of the fitted exponential function or a mean life-time of approx. 5.5 min (see J. Bosbach et al. Contribution to this ISPIV'21).

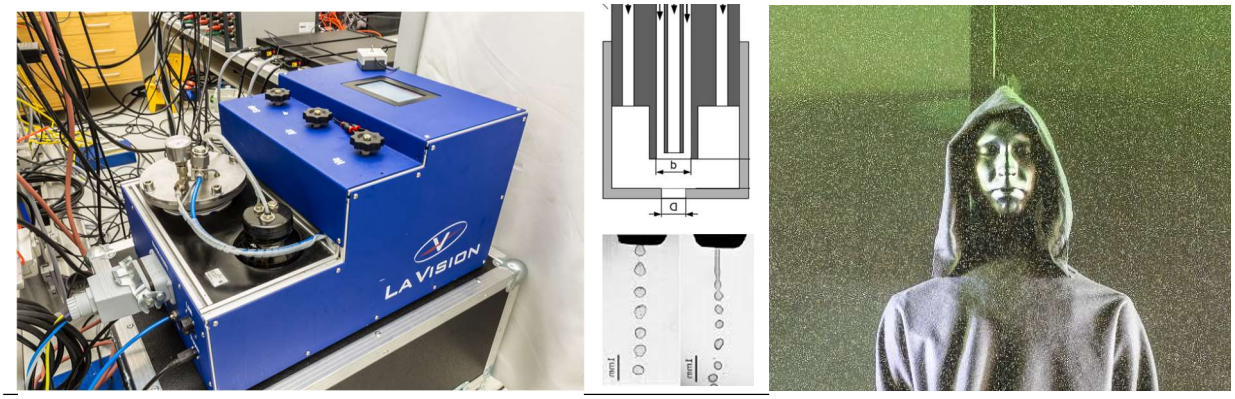

Figure 2: Helium-filled soap bubble (HFSB) generator from LaVision (left), geometry (Bosbach et al. 2009) with shadow graphic images of HFSB nozzle (middle) and cyclically breathing thermal manikin with surrounding illuminated HFSBs (right)

After stopping the HFSB seeding device a waiting time of 2 minutes was always allowed to let the initially disturbed flow to settle down to the internal flow situation basically forced by the breathing cycles and the heated manikin before starting the image acquisition using a DaVis10.x software package. A PTU from LaVision was used for synchronization of the large-scale illumination of the whole room, which was realized by a planar arrangement of various pulsed and collimated LED arrays (9 x Hardsoft ILM-501 (see Stasicki et al 2019), 6 x LED-Flashlight 300 by LaVision and 8 x panels with less dense arranged LEDs (in total 1509 LEDs)) and a back-reflection via a large mirror made of self-adhesive foil from *3M* fixed on a 2 x 2 m² flat wooden plate on the opposite side of the test room. The pulsed light from the array of LEDs had a pulse length of 4 ms each which corresponds to a duty cycle of ~1: 9.6 avoiding smearing effects of the HFSB imaging. The DLR implementation of the Shake-The-Box (STB) method (Schanz et al., 2016) using an advanced Iterative Particle Reconstruction (IPR) code for the "shaking" step and internal loops (Jahn et al. 2021; Wieneke 2013) and the variable time-step STB procedure (VT-STB) (see Schanz et al. contribution to this ISPIV'21) has been applied for the evaluation of the gained time-series of particle images captured by the camera system at between 26 and 28 Hz over time spans of ~52 seconds for each test case. The duration of the time series was limited by the available RAM capacity of the DaVis10 acquisition PC to approximately 1380 time-steps.

The Lagrangian particle trajectories resulting from the STB evaluation allow following between 1.5 and 3 million individual HFSBs in time and space inside the complete volume of the 12 m³ room with a mean position accuracy of ~60 µm. Subsequently, the DLR own data assimilation method FlowFit (Gesemann et al., 2016) has been applied to the dense particle trajectory data which provides the related full time-resolved 3D velocity gradient- and pressure fields.

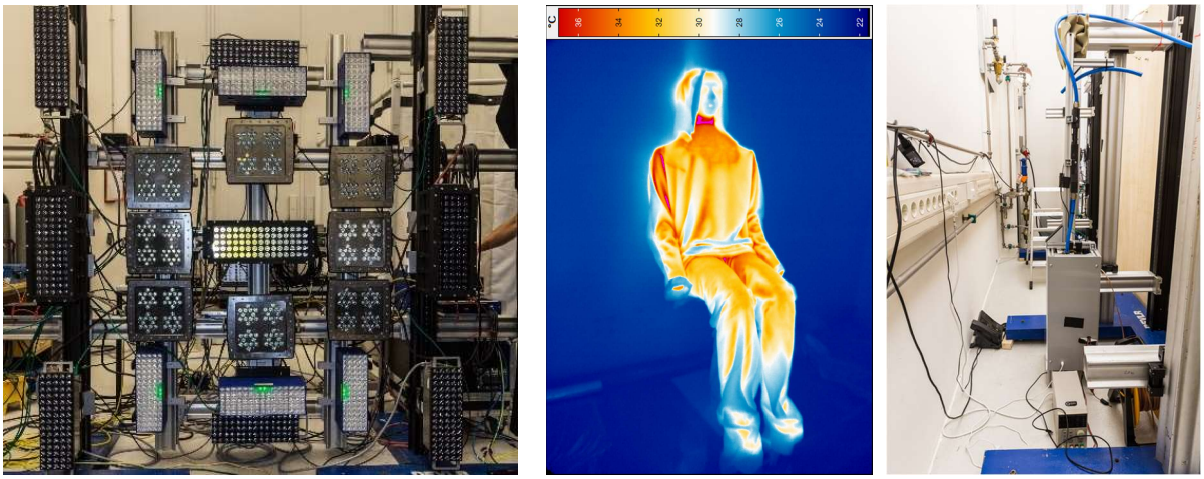

Figure 3: System of LED arrays used for pulsed illumination (left); thermographic image of the heated manikin (middle); breathing apparatus (mechanical lung) (right).

Figure 4: Masks and shields applied for cyclically breathing thermal manikin: Surgical mask (left), transparent face shield (middle) and acrylic glass plate 0.6 m in front of manikin face (right)

The Eulerian representation of the flow fields enables additional insights into the turbulent mixture by the advection of vortical flow structures in the room which are mainly induced by shear flow events generated by the cyclic breathing and the thermal plume above the heated manikin (see Fig. 5 (middle and right)). While during the heavy breathing case, which is sinusoidal breathing at 0.33 Hz with 1.1 liters of volume per breathing cycle, the high momentum jet-like fluid which is cyclically exhaled by our thermal manikin's mouth reaches even the opposite wall at ~1.75 m distance within a few seconds, the same breathing situation with surgical mask applied results in a massive reduction of the horizontal transport of fluid and related aerosol particles. For the situation with mask applied in Fig.5 (bottom-left) the induced pressure loss of the mask enables the HFSBs around the manikin's head to move only slightly as a result ofthe exhaled air. By a small leakage flow of the mask on both sides of the nose the air is partly pushed towards the ceiling (positive y-values) which is also typical for not perfect fitting masks at real humans and well known by people wearing glasses. The exhaled air volume in that case stays in close vicinity of the head and manikin's body and the related HFSBs are transported upwards and get mixed-up with the surrounding air by the vortices of the turbulent thermal plume (see Fig. 5 (middle)) (see for comparison Huhn et al. 2017). Approaching the ceiling the HFSBs trajectories are bended towards a horizontal direction and are transported further in a concentrically way while creating a circular pattern of vortices in the turbulent shear and boundary layer (see Fig. 5 (bottom-left) similar to a low Reynolds number impinging jet (Huhn et al. 2018) which leads to further mixing of the exhaled air with the

surrounding air. While during the heavy breathing case without a mask applied the exhaled air and corresponding aerosol particles reaches the opposite wall (or a hypothetical other person sitting face-to-face in ~1.7 m distance) within a few seconds the pathway of the exhaled air with mask applied gets strongly decelerated at the mask and first travels with the thermal plume towards the ceiling, gets further slowed down and then concentrically distributed along the ceilings surface. After many seconds up to a minute the mixed air with a therefore massively lowered local concentration of exhaled aerosol particles reaches the side walls and starts to descend into the room while creating large low-speed and almost laminar recirculation rollers (see Fig. 5 (bottom-left)). In the case without mask applied high concentrations of horizontally exhaled aerosol particles would directly hit another person's head, which could inhale a critical viral load within a few minutes while on the other hand the mask is not only filtering out many aerosol droplets (depending on the quality of the mask and its tight fitting in the face by ~40 to 90 %) also, those which bypasses the mask would be mixed up in the room and would travel a long way before reaching another person. Any ventilation system would further reduce the viral load in the room and other persons wearing masks would additionally profit from their filter capacities. Of course, wearing masks in a not well-ventilated room would as well cause a critical accumulation of virus laden aerosol particles within several minutes or a few hours depending on the size of the room and the quality of the mask. But the possible residence time for a person in such a scenario before getting infected would be significantly extended.

The void regions related to the heavy breathing cycles in Fig 5 (top-left) signify the fact that the used mechanical lung volume could not be seeded by HFSB and that very fast HFSBs could not be tracked reliably due the low temporal resolution < 28 Hz of the imaging frequency: Displacements of more than 40 pixels in between time-steps have been detected in the exhaled air jet and subsequent strong acceleration events during entrainment of those tracks into vortices in the exhaled air-jet's shear layer poses a main tracking challenge in the present STB evaluation. However, an adaptive tracking system is under development that might account at least partly for this lack of temporal sampling for this small fraction (~0.5 %) of bubbles with respect to the overall reconstructed HFSB tracks.

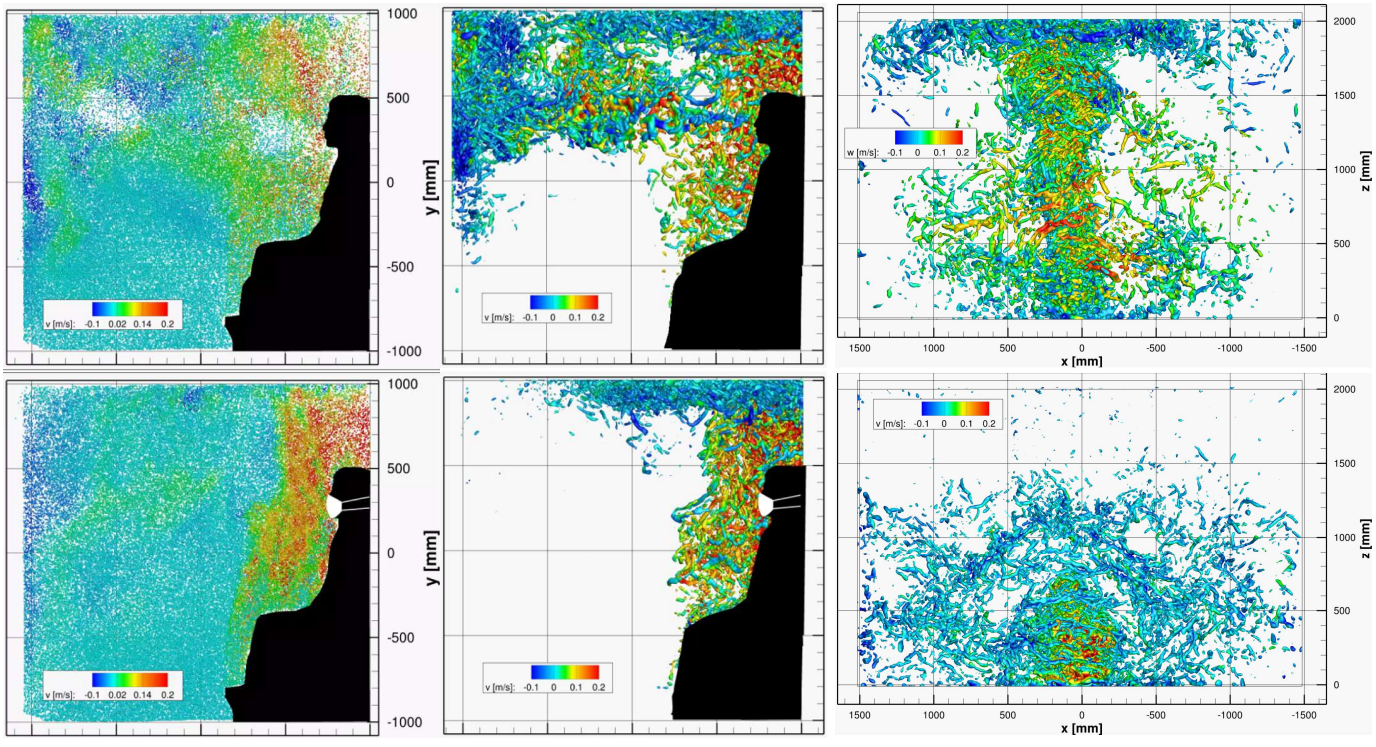

Figure 5: Tracked HFSBs in central 0.24 m slice of the volume, cut from the full extent of 3.0 m (left); related vortical structures in the full 12 m³ volume based on FlowFit data assimilation, sideview (middle), top view (right). Iso-surfaces of Q-values at 6 1/s² colour coded by vertical velocity.

A quite positive effect in terms of aerosol transport pathway deflections and mixing can be described as well for applying an acrylic glass plate with a size of 80 x 80 cm placed almost vertically at ~60 cm distance in front of the mouth of the manikin (see Fig. 6), which is a typical safety measure in small shops, restaurants or at cashier desks in supermarkets. Here, the cyclic exhale-jets of the heavy breathing case impinge on the surface of the vertical glass plate which creates a large ring-like vortex structure with temporally increasing diameter. When this vortex ring is passing over the plates edges the rotational fluid entrains air from the room opposite to the plate towards the manikin which in turn creates a larger recirculation structure on the side of the manikin. Therefore, the exhaled air (and corresponding aerosol particles) gets trapped on the manikins (humans) side of the plate, and it is then mainly further transported by the thermal plume towards the ceiling and distributed in concentrically, partly turbulent pathways along its surface, very similar as for the case with mask applied (see Fig 5). Please keep in mind, that for the case with wearing a face-shield (see Fig. 7) as well as for the vertical plate there are no filter mechanisms acting at the exhaled aerosol particles (beside impingement of large droplets at the face shields surface). Therefore, the overall viral load in the room would still increase unbraked, but for both applied shield methods a fast and direct horizontal transport of aerosol particles with a possible high local concentration towards a hypothetical next person inside the room can be avoided. Any residence of persons over longer time spans would become critical after shorter time-spans compared to the case with masks applied. In order to find a proper measure to indicate critical time spans of personal residences inside populated rooms together with one-spreader one would need information about the whole specific transport and mixing processes, which for our generic test case will be a future postprocessing step on our Lagrangian tracks using information from literature e.g. Lelieveld et al. 2020. Nevertheless, even when assuming isotropic turbulent diffusion with certain time scales, knowing the number of virions exhaled per minute by a spreader and the critical number of inhaled virions for starting an infection at another person allows quite accurately to determine the risk of an infection with an online available calculator (see https://aerosol.ds.mpg.de/en/).

Further coughing and breathing cases have been studied with and without masks and shields applied and the results will be presented in an upcoming journal paper. As mentioned, in a further postprocessing step the full 3D Lagrangian transport processes of potentially infectious exhaled aerosol particles inside the room shall be mimicked and reconstructed with high temporal resolution by using a cyclically increasing subfraction of the HFSBs originating from the exhaled flow volumes. Those will be followed individually during the whole measurement time representing potentially virus laden small bioaerosols. It will allow us to visualize the respective transient and turbulent dispersion process representing an infectious person starting to spread aerosols at the starting point of our measurements. Based on simplifying assumptions further dispersion processes can be studied by extending the time span of one measurement case (~52 seconds or ~12 to 17 breathing cycles) by appending the same volumetric and time-resolved LPT data after the end of a time series temporally and choosing the next closely neighbouring particle in space at the end of each track for extending the statistics towards a few minutes, while newly entering aerosol particles during this time span can be represented by another distinct subfraction of HFSB originating from the exhaled flow volumes.

The gained Lagrangian and Eulerian data from the present study and further postprocessing will be used in a follow-up project supported by the German Research Foundation (DFG). Here the Lagrangian and Eulerian data is used as input and validation data for the development of numerical methods enabling flow simulations and inertial as well as passive aerosol particle dispersions predictions. The developed codes shall be applicable with relatively low computational costs to flow scenarios in more complicated and realistic constellations with additonal dynamics and/or ventilation devices in larger rooms.

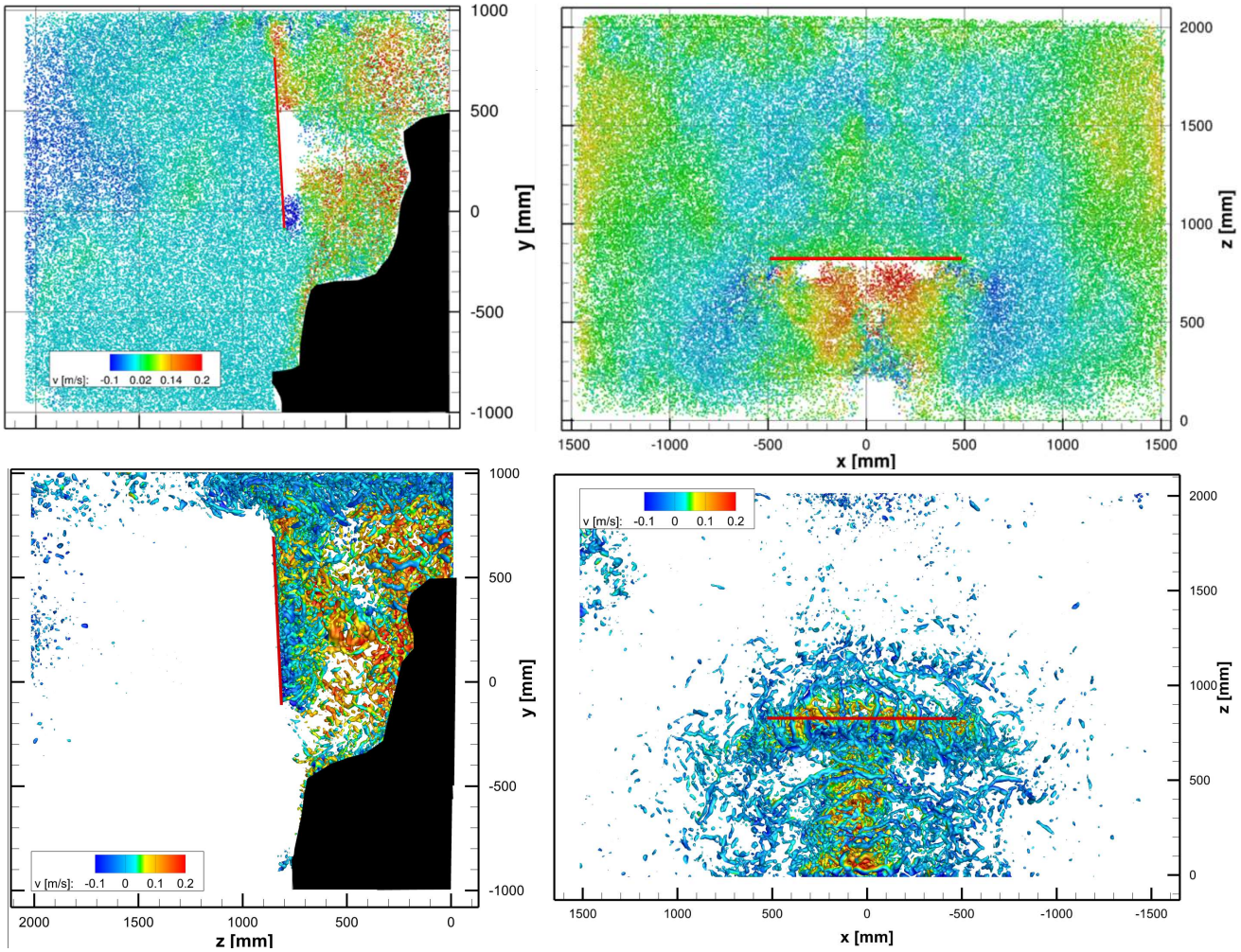

Figure 6: Tracked HFSBs for a heavy breathing case with acrylic glass plate (shown in red) installed 60 cm in front of the manikins' face. Shown are 24 cm deep volume slices each from side view (top-left) and top view (top-right) and corresponding full volume FlowFit results with iso-surfaces of Q-values at 6 1/s²color coded by the vertical velocity (bottom)

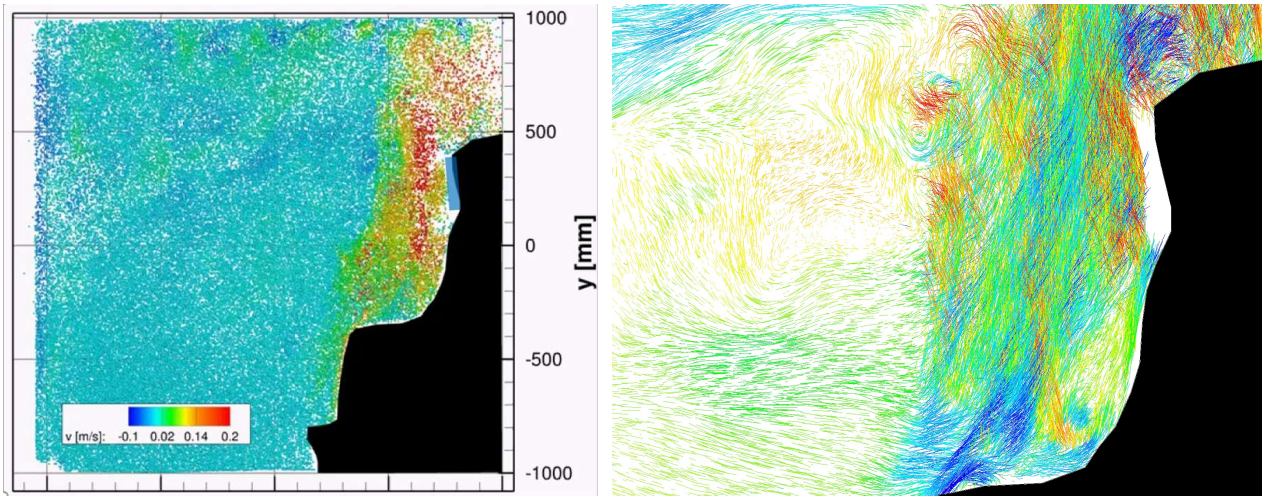

Figure 7: Tracked HFSBs for the heavy breathing case with face shield placed in front of the manikin's face. Shown are 24 cm deep volumes slices of HFSB color coded by vertical velocity (left) and Lagrangian tracks over ~50 time-steps color coded by x -component of acceleration (right) each from sideview

Conclusions

In the present research work an unprecedented large-scale volumetric Lagrangian Particle Tracking (LPT) experiment with up to 3 million instantaneously reconstructed trajectories of submillimeter HFSBs has been performed providing time-resolved velocity and acceleration measurements along all particles' trajectories around a seated and cyclically breathing thermal manikin inside a confined rectangular volume of 12 m³ over a time span of ~52 sec for each case. Assuming nearly neutral buoyancy of small aerosol particles and droplets ($d < 5$ µm) typically exhaled by humans, the nearly neutrally buoyant long-lived HFSBs with ~ 370 µm mean diameter can be considered as their replacements as they act as passive tracers in the present described experimental set-up which is aiming at mimicking a flow situation with a seated person. Full Lagrangian transport processes from various cyclically human breathing and coughing scenarios inside the room with and without masks and shields applied have been captured in 3D with temporal resolution by the DLR in-house Shake-The-Box (STB) evaluation scheme. Only a small selection of the investigated cases could be shown in the present paper. Furthermore, the application of the Navier-Stokes regularized data assimilation scheme FlowFit delivered the complete Eulerian flow field based on the scattered LPT data including the time-resolved 3D velocity gradient tensor- and pressure fields at high spatial resolution. This allows studying the transient and turbulent flow features governing the transport and mixing processes of the small aerosol particles for this generic flow situation in detail. The jet-like cyclically heavy breathing events in case the manikin is not wearing a mask or face shield are the most powerful horizontal transport events in our investigation. On the other hand, the thermal plume of the heated manikin governs the turbulent transport and mixing mechanism in the scenario when protective masks or shields are applied or the breathing is soft. Here, the mean direction of the transport of exhaled aerosol particles is going towards the ceiling, because the decelerated aerosol particles first remain near the body after exhalation. The deceleration and deflection of the exhaled aerosol particles by the investigated mitigation devices is quite advantageous, because the fast horizontal transport of locally highly concentrated aerosol particles and its direct impact at the position of another person is avoided. Nevertheless, over longer time spans an accumulation of aerosol particles occurs in confined rooms without proper ventilation or filtering devices which limits the critical residence time for several persons. Therefore, wearing masks with a high filtration capability of aerosol particles down to diameters ~300 nm (FFP2/3) is highly recommended. Additional shields should be applied in order to separate the flow regimes around individual persons at least for short to intermediate time spans. Unfortunately, the majority of the human population on earth will not be vaccinated during this year and new mutants of SARS-CoV-2 with higher infection rates and/or escape properties are and will be underway. Therefore, the correct application of protective measures (masks and shields) and the detailed understanding of aerosol transport processes in closed rooms are still necessary preconditions for damping the infection risks and chains by optimizing proper technical devices and their application locations (e.g. air purifiers or displacement ventilation systems in buildings, public transport vehicles and air cabins). Finally, the gained knowledge shall give recommendations for human behavior and awareness of critical situations. The complete present Lagrangian and Eulerian flow field data will be used as input for the development of numerical methods allowing to optimizing ventilation systems in closed rooms or transport vehicles with respect to avoiding airborne infection pathways.

Acknowledgements

Support with hard- and software for illumination and image acquisition by LaVision GmbH is gratefully acknowledged. This work was supported by the DFG through Grant SCHR 1165/5-2 in the Priority Programme on Turbulent Superstructures (SPP 1881) and the DLR project Aeromask. Thanks for support of a breathing medical dummy head by OTH Regensburg (Prof. Krenkel). Thanks for technical support at DLR by C. Fuchs, T. Herrmann and T. Kleindienst.

References

Bosbach, J., Kühn, M., Wagner, C. (2009): “Large scale particle image velocimetry with helium filled soap bubbles”. Exp Fluids 46:539–547. https://doi.org/10.1007/s00348-008-0579-0

Cheng, Y., N. Ma, C. Witt, S. Rapp, P.S. Wild, M.O. Andreae, U. Pöschl, H. Su (2021): “Face masks effectively limit the probability of SARS-CoV-2 transmission”. Science, 372:6549, pp. 1439-1443, DOI: 10.1126/science.abg6296 http://science.sciencemag.org/content/early/2021/05/19/science.abg6296

Curtius, J., Granzin, M., Schrod, J. (2020): “Testing mobile air purifiers in a school classroom: Reducing the airborne transmission risk for SARS-CoV-2”. Aerosol Science and Technology, 55:5, https://doi.org/10.1080/02786826.2021.1877257

Van Doremalen, N.; Bushmaker, T.; Morris, D.H.; Holbrook, M.G.; Gamble, A.; Williamson, B.N.; Tamin, A.; Harcourt, J.L.; Thornburg, N.J.; Gerber, S.I.; et al. (2020): “Aerosol and surface stability of SARS-CoV-2 as compared with SARS-CoV-1”. N. Engl. J. Med. 2020, 382, 1564–1567

Fennelly, K. P. (2020): "Particle sizes of infectious aerosols: implications for infection control." The Lancet Respiratory Medicine

Gesemann, S., Huhn, F., Schanz, D., and Schröder, A. (2016): “From Noisy Particle Tracks to Velocity, Acceleration and Pressure Fields using B-splines and Penalties”. 18th Lisbon Int Symp, July 3-7, 2016, Portugal

Huhn, F., Schanz, D., Manovski, P., Gesemann, S., Schröder, A. (2018): “Time-resolved large-scale volumetric pressure fields of an impinging jet from dense Lagrangian particle tracking”. Exp Fluids 59:81, DOI 10.1007/s00348-017-2390-2

Huhn, F., Schanz, D., Gesemann, S., Dierksheide, U., van de Meerendonk, R., Schröder, A. (2017): “Large-scale volumetric flow measurement in a pure thermal plume by dense tracking of helium-filled soap bubbles”. Exp. Fluids 58:116, DOI: 10.1007/s00348-017-2390-2

Jahn, T., Schanz, D., and Schröder, A. (2021): „Advanced Iterative Particle Reconstruction for Lagrangian Particle Tracking”. Submitted for publication at Experiments in Fluids

Johnson, G.R., et al. (2011): “Modality of human expired aerosol size distributions”. Journal of Aerosol Science, 2011. 42(12): p. 839-851

Kähler, C.J., Fuchs, T., Hain, R. (2020): „Können mobile Raumluftreiniger eine indirekte SARS-CoV-2 Infektionsgefahr durch Aerosole wirksam reduzieren?“ DOI: 10.13140/RG.2.2.27503.46243

Kohl, A. (2020): „Entwicklung eines Systems zur experimentellen Simulation der Atmung von Passagieren“. Masterarbeit, TU Ilmenau, https://elib.dlr.de/136986/

Lange, P., Westhoff, A., Schmeling, D., and Dehne, T. (2018): “Low-cost Thermal Manikin - A Competitive Instrument to Simulate Thermal Loads and to Determine Thermal Passenger Comfort”. In: 12th International Manikin and Modelling Meeting, 29.-31. Aug. 2018, St. Gallen, Schweiz

Kupferschmidt, K., and Wadman, M. (2021): „Delta variant triggers new phase in the pandemic”. Science, 372:6549, pp. 1375-1376, DOI: 10.1126/science.372.6549.1375

Liu, J.; Ning, Z.; Chen, Y.; Guo, M.; Liu, Y.; Kumar Gali, N.; Sun, L.; Duan, Y.; Cai, J.; Westerdahl, D.; et al. (2020): “Aerodynamic analysis of SARS-CoV-2 in two Wuhan hospitals”. Nature 2020, 582, 557–560.

Lelieveld, J., Helleis, F., Borrmann, S., Cheng, Y., Drewnick, F., Haug, G., Klimach, T., Sciare J., Su, H., and Pöschl, U. (2020): “Model Calculations of Aerosol Transmission and Infection Risk of COVID-19 in Indoor Environments”. Int. J. Environ. Res. Public Health 2020, 17(21), 8114; https://doi.org/10.3390/ijerph17218114

Mitze, T., Kosfeld, R., Rode, J., and Wälde, K. (2021): “Face masks considerably reduce COVID-19 cases in Germany“, Proc Natl Acad Sci USA 117:51,DOI: 10.1073/pnas.2015954117

Morawska, L., Cao, J., 2020: “Airborne transmission of SARS-CoV-2: the world should face the reality”. Environ. Int. 105730

Morawska, L., Tang, J.W., et al. (2020): "How can airborne transmission of COVID-19 indoors be minimised?" Environ Int 142: 105832.

Schanz, D., Gesemann, S., Schröder, A., Wieneke, B. and Novara, M. (2013): “Non-uniform optical transfer functions in particle imaging: calibration and application to tomographic reconstruction”. Meas. Sci. Tech. 24:024009

Schanz, D., Gesemann, S., and Schröder, A. (2016): “Shake-the-Box: Lagrangian particle tracking at high particle image densities”. Exp Fluids 57:70, 2016, DOI 10.1007/s00348-016-2157-1

Schanz D, Schröder A, Novara M, Geisler R, Agocs J, Eich F, Bross M, and Kähler CJ (2019) Large-scale volumetric characterization of a turbulent boundary layer flow. in Proceedings of the 13th International Symposium on Particle Image Velocimetry. 182. pages 251–265. Universität der Bundeswehr München: AtheneForschung

Stasicki B, Schröder A, Boden F, and Ludwikowski K (2017): “High-power LED light sources for optical measurement systems operated in continuous and overdriven pulsed modes”. in Optical Measurement Systems for Industrial Inspection X. volume 10329. page 103292J. International Society for Optics and Photonics

van Doremalen, N., Bushmaker, T., Morris, D.H., Holbrook, M.G., Gamble, A., Williamson, B.N., et al. (2020): “Aerosol and surface stability of SARS-CoV-2 as compared with SARS-CoV-1”. N. Engl. J. Med

Wieneke B (2008): “Volume self-calibration for 3D particle image velocimetry”. Exp. Fluids 45:549–556

Wieneke B (2013): “Iterative reconstruction of volumetric particle distribution”. Meas. Sci. Tech. 24:024008

Zuo, Y.Y., Uspal, W.E., Wei, T. (2020): “Airborne Transmission of COVID-19: Aerosol Dispersion, Lung Deposition, and Virus-Receptor Interactions”. ACS Nano 2020 14 (12), 16502-16524